Available online at www.sciencedirect.com

SciVerse ScienceDirect

Journal of Magnesium and Alloys 1 (2013) 94−100
www.elsevier.com/journals/journal-of-magnesium-and-alloys/2213-9567

Full length article

The effect of addition of Nd and Ce on the microstructure and mechanical properties of ZM21 Mg alloy

Binjiang Lv [a], Jian Peng [a,b,*], Yi Peng [a], Aitao Tang [a]

[a] College of Materials Science and Engineering, Chongqing University, 400044, China
[b] Chongqing Academy of Science and Technology, Chongqing 401123, China

Abstract

The microstructures and mechanical properties of Mg−2.0Zn−1.0Mn (ZM21) alloys with certain amount of Ce and Nd additions were investigated, and the influence mechanism of Ce and Nd on the microstructures and mechanical properties of extruded alloys was discussed. The results indicated that the addition of Nd and Ce can refine the grains in ZM21 alloy, for which the distribution density of second phase particle played a major role to hinder the growth of dynamic recrystallization (DRX) grain in alloys by adding a content of 0.4 wt.% Ce and Nd. The average grain size of ZM21 alloy with the additions of 0.4 wt.% Nd and Ce reached 6 ± 3 μm and 13 ± 2 μm, respectively. Adding Ce and Nd to ZM21 alloy, the changes of mechanical properties were mainly attributed to a reduction in basal texture intensity, refinement grain size as well as the dispersion density and distribution position of fine second phase particles. Furthermore, by addition of Ce and Nd to ZM21 alloy, the non-basal plane slip system could be activated which decreased the basal texture intensity.

Keywords: Microstructure; Mechanical properties; Second phase

1. Introduction

Magnesium alloys are used in a wide range due to their low density, good formability, favorable recycling capability and excellent damping capacity [1,2]. Mg−Zn serial alloys become a research focus for their high strength, good plasticity and processing performance [3,4]. However, Mg−Zn serial alloys take the disadvantages of difficult grain refinement and easy to produce loose defects, which limits the application of industrial castings and deformation products [5]. ZM21 (Mg−2.0Zn−0.3Zr) has the advantages of low alloying and rapid thermal processing forming that is commonly used as a commercial Mg alloy [6−8]. However, the mechanical properties of ZM21 alloy still cannot satisfy the requirements of some important application fields.

The hcp crystal structure of Mg alloy can lead to form a strong {0001} basal texture during the deformation process, which deteriorates the secondary deformation forming ability of Mg alloy [9,10]. The addition of Nd and Ce could refine the grain size and improve the mechanical properties of Mg alloy. It is well known that the additions of rare earth (RE) elements such as Nd and Ce in Mg−Zn based alloys can significantly affect the mechanical properties [11−14]. Unfortunately, those studies about the addition of Nd and Ce are concerned in high Zn content alloy. LE Qichi's research [15] indicated that an addition of 0.4 wt.% Nd and Ce could significantly improve the elongation and strength of Mg−2.0Zn alloy, respectively. However, the mechanism of the effect on mechanical

* Corresponding author. College of Materials Science and Engineering, Chongqing University, 400044, China. Tel.: +86 23 6511 2291; fax: +86 23 6510 2710.
E-mail address: jpeng@cqu.edu.cn (J. Peng).
Peer review under responsibility of National Engineering Research Center for Magnesium Alloys of China, Chongqing University

Production and hosting by Elsevier

http://dx.doi.org/10.1016/j.jma.2013.02.011

Table 1
Chemical component and secondary phase volume fraction of the alloy (wt%).

Alloy no.	Composition (wt.%)				
	Zn (wt.%)	Mn (wt.%)	Ce (wt.%)	Nd (wt.%)	Mg
ZM21	1.9	1.0	–	–	Bal
ZM21–0.4Nd	1.9	0.9	–	0.4	Bal
ZM21–0.4Ce	1.8	0.9	0.4	–	Bal

properties with an addition of Nd and Ce in low Zn content Mg–2.0Zn alloy is still not totally clear. Especially, the influence mechanism of Ce and Nd rare earth elements on the microstructures and mechanical properties of ZM21 extruded alloy is rarely discussed.

The present work aimed to investigate the effect of a same content addition of Nd and Ce on the microstructures and tensile properties of ZM21 extruded alloy at room temperature. The influence mechanism of Ce and Nd are discussed by comparing the mechanical properties and microstructures of ZM21 alloy with Nd and Ce added ZM21 alloy.

2. Experimental procedures

The materials used in this study were the as-cast magnesium alloys with different rare earth element contents, which were prepared by a water-cooled semi-continuous casting system in CCMg in Chongqing University, China. The chemical compositions of the studied alloys are shown in Table 1. The materials used in this study were made from pure Mg (99.98%), melted in a 60 KW resistance furnace to which pure Zn (99.9%), Mg–Mn (3.9 wt.%) master alloy, Mg–Nd (20 wt.%) master alloys and Mg–Ce (20 wt.%) master alloys were added under the protection of a CO_2 (1 vol.%) and SF_6 (99 vol.%) mixed gas atmosphere. When the temperature reached 750 °C, molten metal was stirred for 5 min, keeping for 30 min at 720 °C, then molten alloys were cast into cylindrical ingots 92 mm in diameter and 800 mm in length, and the chemical compositions were tested by ARL4460 optical spectrometer. The cast ingots were homogenized by annealing at 420 °C for 12 h and then hot-extruded into rods with a diameter of 16 mm. The extrusion ratio was 28, and the ingot temperature was 420 °C.

As-cast alloys were etched with an etchant (glycerol + hydrochloric acid + acetic acid + nitric acid). Extruded alloys were etched with an etchant (5 g picric acid, 10 ml acetic acid and 70 ml alcohol). Microstructures of the investigated extruded alloys were determined by optical microscope (OPTEC, MDS) and scanning electron microscope (SEM, TESCAN VEGA II LMU) with energy dispersive spectroscopy (EDS). The grain sizes were estimated by IPP (Image Pro-Plus). Phase analyzes were carried out by X-ray diffraction with a Cu target (Rigaku D/Max-2500PC). Extruded samples were machined into tensile specimens of 8 mm gage diameter and 40 mm gage length. Tensile testing was performed at room temperature on the CMT-5105 electronic universal testing machine with a cross-head speed of 3 mm/min.

3. Results and discussion

3.1. The effect of Nd and Ce on microstructure of ZM21 alloy

Fig. 1 shows the color metallography images of as-cast alloy specimen. The as-cast alloy exhibits a grain coarsening with a content of 0.4 wt.% Nd addition, as shown in Fig. 1(b). The average grain size of as-cast ZM21 alloy is 323 ± 56 μm,

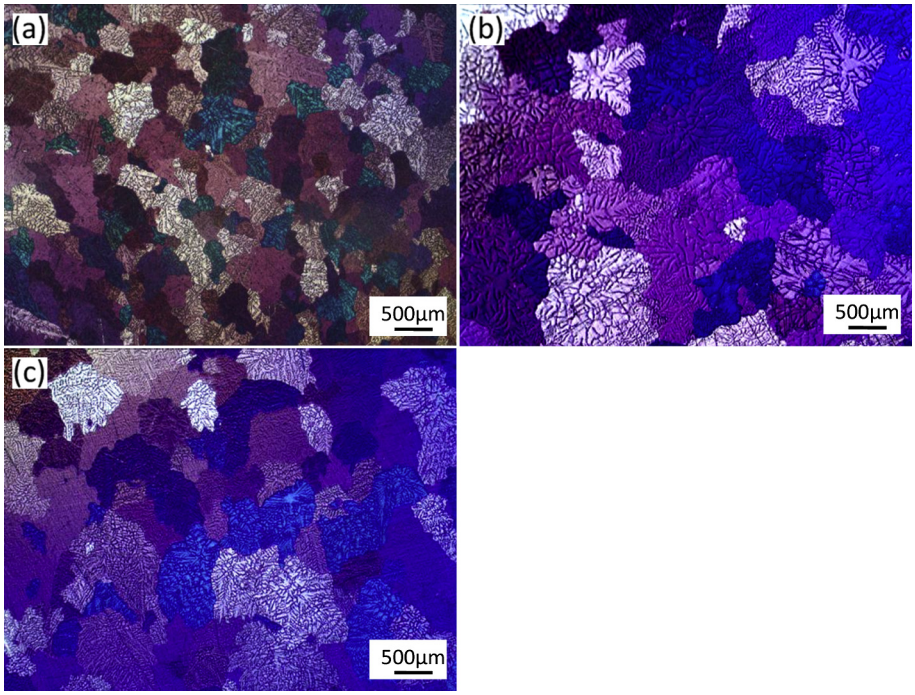

Fig. 1. Color metallography images of as-cast alloys (a) ZM21 (b) ZM21–0.4Nd (c) ZM21–0.4Ce.

which increases to 650 ± 80 μm by adding a content of 0.4 wt.% Nd. Adding a same content of Ce, the grains in ZM21−0.4Ce alloy are coarsened as well as ZM21−0.4Nd alloy with an average grain size of 514 ± 67 μm.

Fig. 2 is the microstructure photographs and the normal distribution of grain size of extruded alloy. The average grain size of extruded ZM21 alloy is 18 ± 6 μm. The grain size decreases with the addition of Nd and Ce element. The average grain size of ZM21−0.4Nd and ZM21−0.4Ce alloy reaches 13 ± 4 μm and 6 ± 2 μm, respectively. The uniformity of grain size of ZM21−0.4Nd is much better than that of ZM21 and ZM21−0.4Ce alloy. Adding the same mass fraction of Nd, Ce rare-earth element in ZM21 alloy can significantly refine the DRX grain, to which Ce plays a more important role than Nd. After extrusion process deformation, the second phases distributing in the matrix and grain boundaries that is shown in Fig. 2a, b & c.

The XRD patterns of extruded alloys are shown in Fig. 3. As the solubility of Zn in Mg is 6.2 wt.% at room temperature, for the Zn content 2 wt.% in ZM21 alloy, Zn element is all dissolved in the Mg matrix of ZM21 alloy. There is no Mg−Zn compounds, and only a small amount of Mn dispersed in the matrix as simple substance phase (Fig. 2a). After adding 0.4 wt.% Nd, two ternary phases T_2 ($(Mg,Zn)_{11.5}Nd$)and T_3 ($(Mg,Zn)_3Nd$) are formed in ZM21 alloy. Two second phases $Mg_{17}Ce_2$ (Hexagonal structure) phase and T-phase (Orthorhombic)are formed in

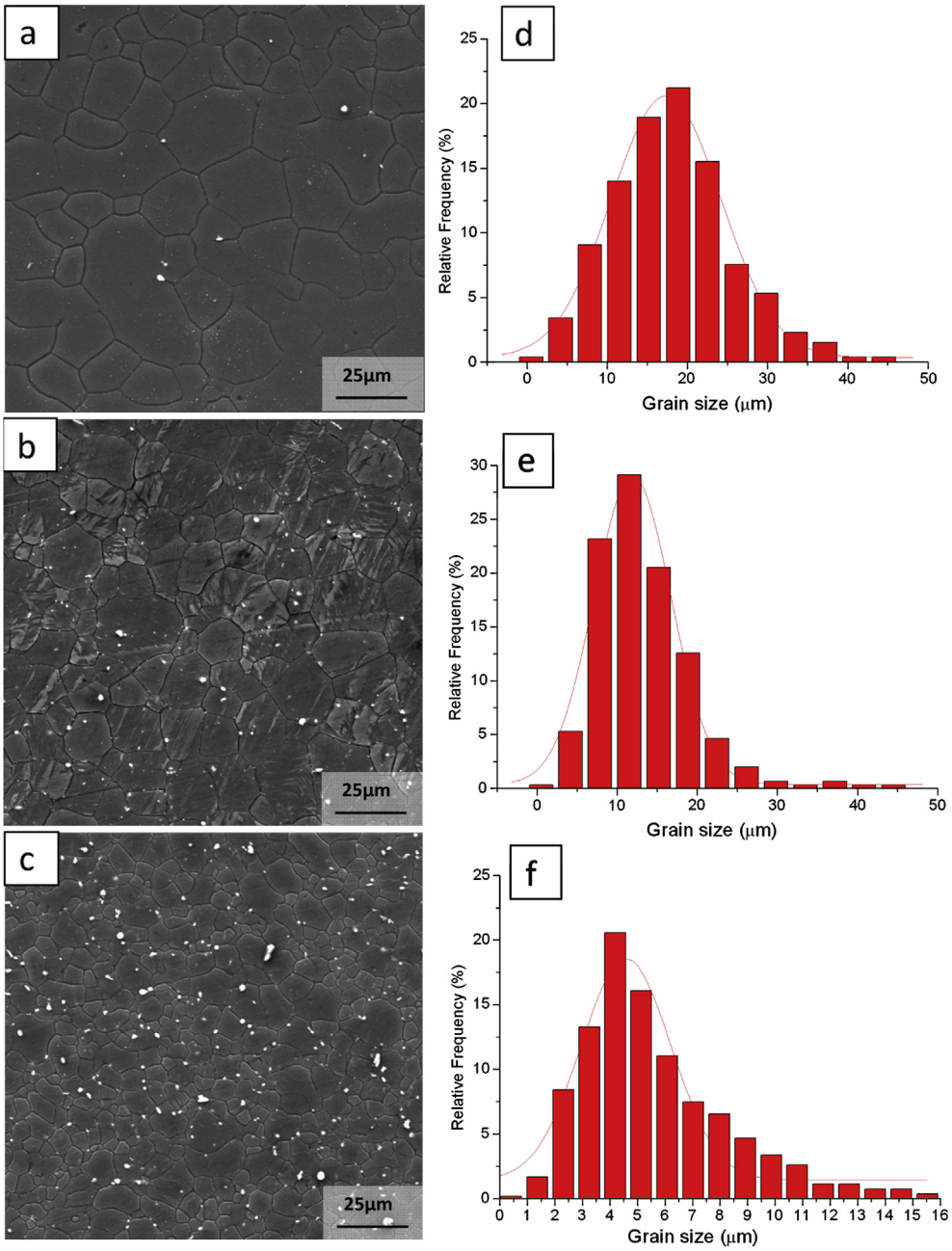

Fig. 2. The microstructure photographs and the normal distribution of grain size of extruded alloys. (a & d) ZM21 (b & e) ZM21−0.4Nd (c & f) ZM21−0.4Ce.

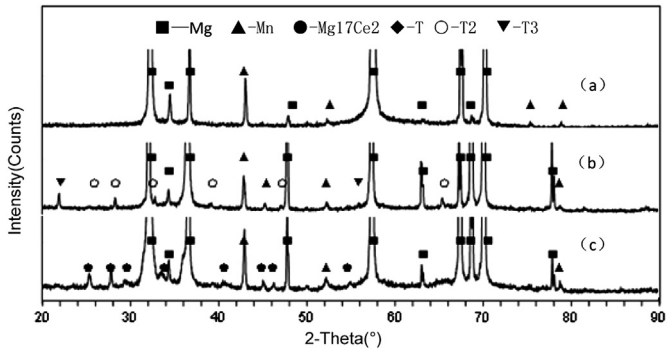

Fig. 3. XRD analysis of alloys (a) ZM21 (b) ZM21−0.4Nd (c) ZM21−0.4Ce.

ZM21−0.4Ce alloy. After extrusion deformation, the second phase with globular structure distributing in the matrix and grain boundaries, as shown in Fig. 2(a, b & c).

3.2. The effect of Nd and Ce on mechanical properties of extruded ZM21 alloy

The tensile tests of extruded alloys at room temperature are shown in Table 2. With addition of 0.4 wt.% Nd into ZM21 alloy, the UTS and YS both decrease compared with ZM21 alloy. However, the elongation of ZM21−0.4Nd alloy is significantly improved with a max value of (28.8 ± 2)%. Conversely, The UTS and YS both increase by adding 0.4 wt.% Ce, and the elongation reaches a value of 19.2 ± 0.4% which is much lower than that of ZM21−0.4Nd alloy.

The {0001} pole figures of extruded alloys are shown in Fig. 4. The {0001} basal texture is formed in ZM21 alloy after extrusion deformation. The max texture intensity of ZM21 alloy reaches 4.6. The texture intensity reduces significantly in ZM21−0.4Nd alloy caused by Nd addition, of which the max value is only 2.2. By adding Ce into ZM21 alloy, the texture intensity of extruded alloy also reduces (the max texture intensity is 2.0). As shown in Fig. 4, the {0001} basal texture was formed in extruded alloys, and the intensity of basal texture become lower by the addition of Nd and Ce. In addition, there are apparent peak intensity between (0001) and $(11\bar{2}0)$, even the peak intensity between (0001) and$(10\bar{1}0)$, which suggests the activation of non-basal slip system.

As shown in Fig. 5(a, b & c), Few twins are formed in those three extruded alloy specimens. The longitudinal profiles of tensile fracture with the stretch rate of 3 mm/min are shown in Fig. 5.Many twins are present in ZM21 alloy during tensile test at room temperature. There are some twins in ZM21−0.4Nd alloy, but the quantity is less than that in ZM21 alloy. However, only few twins are present in ZM21−0.4Ce alloy. Meyers

Table .2
Mechanical properties of extruded alloy.

Alloy no.	Mechanical properties		
	UTS (MPa)	YS (MPa)	EL (%)
ZM21	251 ± 1.2	171 ± 0.9	13.7 ± 0.1
ZM21−0.4Nd	235 ± 0.7	148 ± 1.1	28.8 ± 2.0
ZM21−0.4Ce	261 ± 0.8	185 ± 0.6	19.2 ± 0.4

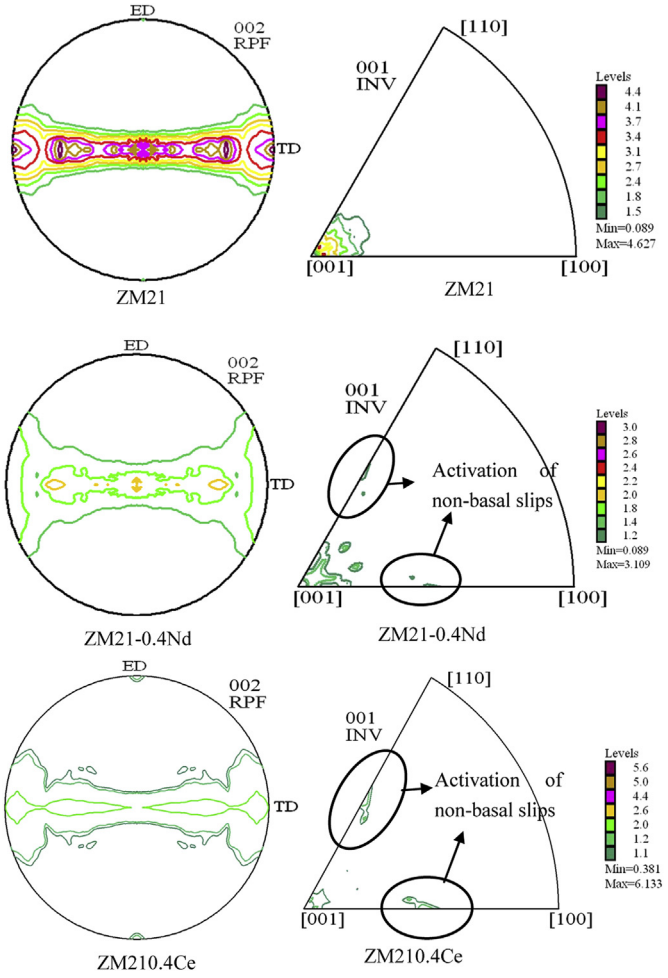

Fig. 4. {0001} pole figures and inverse pole figures of extruded alloys.

M.A [16] indicated that twinning mainly occurred in coarse grains. The distance of dislocation slip in coarse grains is long enough to cause severe stress concentration near the grain boundary, which is necessary to initial twinning. The probability of twining reduced which was attributed to the grain refinement. Grain refinement decreases the dislocation glide process, which makes the alloy mainly depend on the cross-slip, non-basal slip, GBS and dynamic recovery to release the stress concentration, and the stress state is difficult to meet the twin requirements of the twining nucleus.

4. Discussions

4.1. The effect of Ce and Nd on microstructures of extruded alloys

The microstructures of as-cast alloys are coarsen by the addition of 0.4 wt.% Nd and Ce. After extrusion deformation, many fine particles distribute in the matrix and grain boundaries of extruded ZM21 alloys with Nd and Ce addition, and the grains are refined significantly. The average diameter and distribution density of second phase particles were count by IPP. The average diameter of second phase particles is 0.8 ± 0.67 μm, of which the distribution density is 15,834/mm^2 in ZM21−0.4Nd alloy;

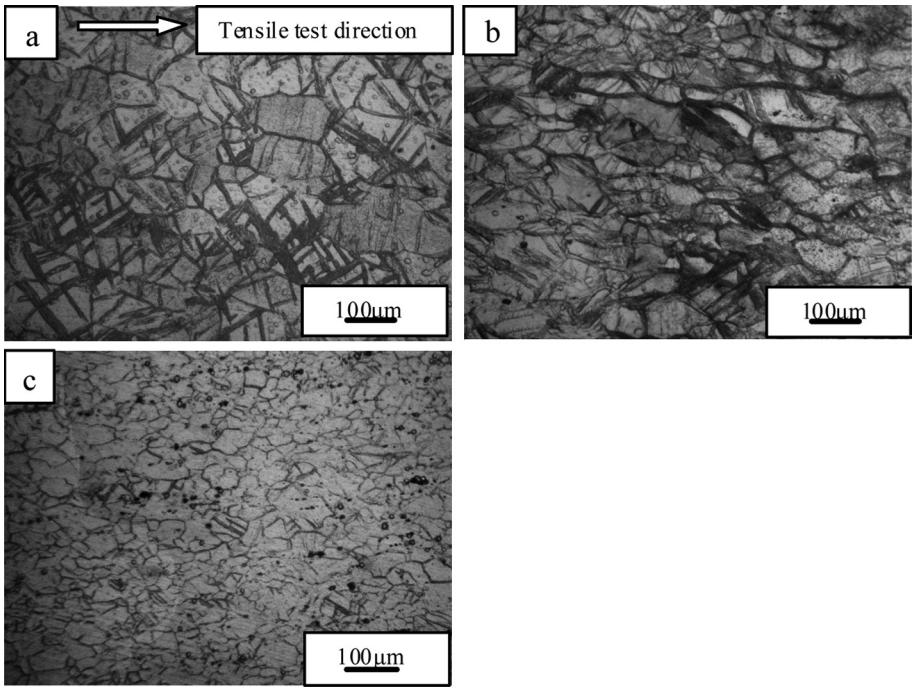

Fig. 5. The longitudinal profiles near tensile fracture a) ZM21 b) ZM21−0.4Nd c) ZM21−0.4Ce.

the average diameter and distribution density of second phase particles in ZM21−0.4Ce is 0.8 ± 0.64 μm and 26,923/mm^2, respectively.

It is well known that the resistance of second phase particles on grain boundary can be expressed as [17,18]:

$$R = K \cdot \frac{r}{f} \tag{1}$$

K is a constant, r is the radius of second phase particles, f is the volume fraction of second phase. According to statistical results, the radius of second phase particles in ZM21−0.4Nd is basically equal to that in ZM21−0.4Ce, and second phase particle distribution density of ZM21−0.4Ce alloy is about 1.8 times than that of ZM21−0.4Nd alloy. Obviously, the resistance of second phase particles in grain boundary enhances with the increase of fine particles volume fraction. When the second phase particles distribute on grain boundaries, they occupy the grain boundary, which reduces the total grain boundary energy, and grain boundary motion is pinned by the second phase particles on the grain boundary [19−21].

4.2. The influence mechanism of Nd and Ce on mechanical properties of ZM21 alloy

Fine second phases particles with globular structure that distribute in the matrix and grain boundaries, which have a dispersion strengthening effect on extruded alloys.

For dispersion strengthening of fine particle obstacles, the Orowan increment in CRSS produced by the need for dislocations to bypass these obstacles is given as [22−25]:

$$\Delta\tau = \frac{Gb}{2\pi\lambda\sqrt{1-\nu}} \ln\frac{d_p}{r_0} \tag{2}$$

where Ds the increment in CRSS due to dispersion strengthening, G the shear modulus of the magnesium matrix phase, b the magnitude of the Burgers vector of the slip dislocations, ν the Poisson's ratio k the effective planar inter-obstacle spacing, d_p the mean planar diameter of the point obstacles, and r_0 is the core radius of dislocations.

d_1 is a triangular array of spherical particles of uniform diameter, and the effective planar inter-precipitate spacing is calculated as [26] :

$$\lambda = \left(\frac{0.779}{\sqrt{f}} - 0.785\right) d_1 \tag{3}$$

where f the volume fraction of fine particles, then the equation can be written as [26]:

$$\Delta\tau = \frac{Gb}{2\pi\sqrt{1-\nu}\left(\frac{0.779}{\sqrt{f}} - 0.785\right) d_1} \ln\frac{0.785 d_1}{b} \tag{4}$$

According to equation (4), the value of G, ν and b is steady, the dispersion strengthening effect enhances with increase of the second phase particles volume fraction. The radius of fine particles in ZM21−0.4Nd is equal to that in ZM21−0.4Ce. As a result, the greater the density of second phase particles, the larger the volume fraction becomes. The relationship of fine particles distribution density between three extruded alloys is as following:

$f_{ZM21-0.4Ce} > f_{ZM21-0.4Nd} > f_{ZM21}$

Thus, the order of the distribution strengthening effect is :

$$ZM21 - 0.4Ce > ZM21 - 0.4Nd > ZM21$$

Grain size of ZM21 alloy is refined significantly with Nd and Ce addition. According to the well-known Hall−Petch relationship, the yield strength depends on the grain size [27,28] :

$$\sigma_y = \sigma_0 + Kd^{-1/2} \quad (5)$$

σ_0 and K are constant and d is the grain size and d is a measure of the grain diameter. The higher density of grain boundaries due to smaller grain sizes can act as an effective obstacle to the dislocation propagation. This is why grain refinement by the DRX process can increase the yield strength. For order of d:$d_{ZM21-0.4Ce} < d_{ZM21-0.4Nd} < d_{ZM21}$, thus, the order of fine grain strengthening is must as following :

$$ZM21 - 0.4Ce > ZM21 - 0.4Nd > ZM21$$

As shown in Fig. 4, {0001} basal texture intensity decreases with Nd and Ce content of 0.4 wt.%. The {0001} basal texture which is parallel to the extrusion direction is the mainly texture in magnesium alloy. When the direction of tensile test is parallel to the extrusion direction, the Schmid factor of grains' basal plane slip system is zero, which enhances the strength of extruded alloys. The texture strengthening effect on extruded alloys is decreased which is attributed to a decrease of basal texture intensity. The order of the {0002} basal texture intensity component is:

$$ZM21 > ZM21 - 0.4Nd > ZM21 - 0.4Ce$$

The order of texture strengthening effect is:

$$ZM21 > ZM21 - 0.4Nd > ZM21 - 0.4Ce$$

In summary, the fine grain strengthening effect and dispersion strengthening effect in ZM21−0.4Nd alloy are stronger than those in ZM21 alloy. However, the texture strengthening effect in ZM21−0.4Nd alloy is much more weaken than that in ZM21 alloy; the strength of ZM21−0.4Nd is decreased, which indicates that the texture strengthening effect plays an important role in ZM21 alloy. The basal texture intensity of ZM21 alloy is almost the same by adding Ce or Nd. However, the UTS and YS of ZM21−0.4Ce alloy is much higher than those of ZM21−0.4Nd alloy, which implies that the main factors affecting the strength are distribution strengthening and fine grain strengthening caused by adding Nd and Ce elements.

4.2.1. The effect of Nd and Ce on plasticity of ZM21 alloy

The intensity of {0001} basal texture in ZM21 alloy with Nd content of 0.4 wt.% is weakened significantly. The existence of {0001} basal texture is the main reason for poor plasticity in room temperature because weakening the {0001} basal texture can improve the plasticity and toughness of the alloy at room temperature. During tensile testing along the extrusion direction, some of the grains' basal plane along the extrusion direction produces a deflection with a certain angle. Compared to ZM21 extruded alloy, the base surfaces' Schmid factors of ZM21−0.4Nd alloy is much bigger. The basal panel lie in soft orientation is good for plastic deformation. The grain size was refined by the Nd addition. The grain boundary area per unit volume increases as the grain refinement. The plasticity of the ZM21−0.4Nd alloy was improved results from the increasing of dislocations and cracks formation energy. As shown in Fig. 5, many twins formed in ZM21 alloy after tensile test. There is a certain amount of twins in ZM21−0.4Nd alloy at the stretching rate of 3 mm/min, which further improves the elongation of ZM21−0.4Nd alloy. In previous study [29], twins mainly formed in coarse grain, and the slip distance of dislocation increased to produce a severe stress concentration at the boundaries. The twins can adjust the crystal orientation and release the stress concentration during the tensile deformation process, which further stimulate slip to make the slip and twin be carried out alternately. Therefore, when the average grain size is 6 ± 2 μm, slip is the main deformation mechanism of the alloy; while the average grain size of between 13 ± 4 μm and 18 ± 6 μm, the twinning deformation mechanism is changed into slip deformation mechanism.

The elongation of ZM21 alloy is improved by adding a content of Y addition, of which the influence mechanisms are as follows: 1)The Ce addition decreased texture intensity of {0001} basal texture, which was lower than that of ZM21 alloy. 2) The grain size was refined so that it can improve the plasticity of ZM21−0.4Ce alloy. 3) The grain in ZM21−0.4Ce alloy is very fine with a dimension of 6 ± 2 μm. Grain refinement can inhibit the formation of twins [29]. The number of twins decreased in ZM21−0.4Ce alloy, which makes the elongation of ZM21−0.4Ce alloy lower than that of ZM21−0.4Nd alloy. 4) Adding the same amount of Nd and Ce into ZM21 alloy, the intensity of basal texture of ZM21 alloy is basically decreased, but the elongation of ZM21−0.4Ce alloy is lower than ZM21−0.4Nd alloy. The fine second phase particles distributing along the grain boundaries could hinder the dislocations motion that create a high dislocation density and stress concentration in the grain-boundary region to become crack sources, which could decrease the plasticity of alloy. The distribution density of second phase particles in ZM21−0.4Nd alloy is larger than it in ZM21−0.4Ce alloy, and 85% of fine particles distributed on the grain boundaries, which leads to initiation of fracture at the boundaries to decrease the plasticity of ZM21−0.4Ce alloy. As we have seen, twining does not play an important role to crystal plastic deformation for the shear deformation of twin is generally far less than the slip deformation during the plastic deformation process. The distribution density and distribution position of fine second particles significantly affect the plasticity of alloy. It is for this reason that the elongation of ZM21−0.4Ce alloy is lower than ZM21−0.4Nd alloy.

4.3. The effect of Nd and Ce on texture in ZM21 alloys

The intensity of basal texture of ZM21 alloy decreased with Nd and Ce addition, which improved the plasticity of extruded alloys. Texture is one of the most important effects on

Table 3
Lattice parameter of homogenized alloys.

Sample	a (nm)	c (nm)	c/a
ZM21	0.32122	0.52121	1.62260
ZM21−0.4Nd	0.32124	0.52169	1.62399
ZM21−0.4Ce	0.32059	0.52034	1.62307

mechanical properties of ZM21 alloys. The basal texture decreasing is the basic reason why non-basal plane slip system is activated. The addition of Nd and Ce does not result in a decrease of c/a ratio. On the contrary, the c/a ratio is slight increased by adding same mass fraction of Nd and Ce, of which the result was shown in Table 3. The low of the change of c/a ratio by adding Nd and Ce was reported by Yasumasa Chino [30], which indicated that the activation of non-basal slip does not stem from the change of crystal structure. Koike et al. [31] reported that grain refinement is effective for the enhancement of ductility because of the activation of the non-basal slips near the grain boundaries, resulting from the stress concentration at the grain boundaries. The activation of non-basal slip decreased the intensity of basal texture.

5. Conclusions

1) By the addition of 0.4 wt.% Ce and Nd, the radius of the second phase particles in ZM21−0.4Nd is basically equal to it in ZM21−0.4Ce, and the distribution density and distribution position of second phase particles play a very important role in grain refinement. The grain refinement ability of Ce is better than Nd with same mass fraction content.
2) The tensile strength of ZM21 with a content of 0.4 wt.% Nd decreased because that the influence of decreasing of texture strengthening is stronger than grain refinement strengthening and dispersion strengthening; the grain refinement strengthening and dispersion strengthening of Ce is stronger than Nd, which increased the tensile strength of ZM21 with same content of 0.4 wt.% Ce.
3) Adding Nd element into ZM21 alloy, the plasticity of ZM21 increased significantly are attribute to the decreasing of basal texture, grain refinement and compatible deformation of twins during deformation process. The effect of texture weakening and grain refinement of Ce is stronger than Nd, on the contrary, the elongation of ZM21 with Ce addition is lower than ZM21 alloy with same content of Nd because that most of second phase particles distributed in the grain boundaries, which cause a high dislocation density and crack resource to decrease the plasticity of alloy.
4) The c/a ratio is slightly increased by adding Ce and Nd, which indicates that the activation of non-basal slip system are not attributed to the change of the c/a ratio.

Acknowledgments

This work was supported by the National Science & Technology Support Program (Project No. 2011BAE22B03-3), International Science & Technology Cooperation Program of China (2011DFA5090), Chongqing Key Science and Technology Projects (CTSC-2010AA4045) and Nature Science Foundation Project of CQ (CSTS-2010BB4068).

References

[1] L.H. Chen, H.J. Zhao, Z. Liu, Foundry 10 (1999) 45.
[2] H. Friderich, S. Schumann, Mater. Sci. Technol 117 (1) (2001) 276.
[3] D.K. Xu, L. Liu, Y.B. Xu, et al., Journal of Alloys and Compound 426 (2006) 155−161.
[4] H. Watanabe, T. Mukai, Scripta Materialia 41 (2) (1999) 209−213.
[5] Z. Yang, J.P. Li, J.X. Zhang, et al., Acta Metallurgica Sinica 21 (5) (2008) 313−328.
[6] Bohlen Jan, Letzig Dietmar, K.U. Jauber, Metals and Materials Society (5) (2007) 95−100.
[7] Mohamad El Mehtedi, Luigi Balloni, S. Spigarelli, E. Evangelista, G.I. Rosen, Key Engineering Materials 367 (2008) 79−86.
[8] Dale Latwell, Matthew R. Barnett, Metallurgical and Materials Transactions A 38 (12) (2007) 3032−3041.
[9] Zhen-hua Chen, Wei-jun Xia, Yong-qi Chen, Ding-f Fu, The Chinese Journal of Nonferrous Metals 15 (1) (2005) 1−11.
[10] Guo Qiang, Yan Hongge, Chen Zhenhua, Yuanzhi Wu, Jie Chen, Acta Metallurgica Sinica 43 (6) (2007) 619−624.
[11] K. Yu, X.Y. Wang, S.T. Rui, et al., Journal of Central South University of Technology 15 (2008) 434−437.
[12] Wenjiang Ding, Daquan Li, Qudong Wang, Qiang Li, Materials Science and Engineering A 483−484 (2008) 228−230.
[13] J. Yang, J.L. Wang, L.D. Wang, et al., Materials Science and Engineering A 479 (2008) 339−344.
[14] Kun Yu, Wenxian Li, Jun Zhao, Zhengqing Ma, Richu Wang, Scripta Materialia 48 (2003) 1319−1323.
[15] Le Qi-chi, Zhang Zhi-qiang, Shao Zhi-wen, Cui Jian-zhong, Xie Yi, Transactions of Nonferrous Metals Society of China 20 (2010) s352−s356.
[16] M.A. Meyers, O. Vohringer, V.A. Lubarda, Acta Mater 49 (2001) 4025−4039.
[17] F. Weinberg, Progress in Metal Physics 8 (1959) 105−128. IN7, 129−146.
[18] D. McLean, Grain Boundaries in Metals, Clarendon Press, 1957.
[19] Z.X. Wang, J.X. Xie, X.F. Liu, J.Y. Li, D.F. Zhang, F.S. Pan, Acta Metallurgica Sinica 43 (2007) 920−924.
[20] A. Galiyev, R. Kaibyshev, G. Gottstein, Acta Materialia 49 (2001) 1199−1207.
[21] N. Stanford, M. Barnett, Scripta Materialia 58 (2008) 179−182.
[22] L.M. Brown, R.K. Ham, in: A. Kelly, R.B. Nicholson (Eds.), Strengthening Methods in Crystals, Elsevier Pub-lishing Company, London, 1971, p. 12.
[23] A.J. Ardell, Metallurgical and Materials Transactions A 16A (1985) 2131−2165.
[24] E. Nembach, Particle Strengthening in Metals and Alloys, John Wiley & Sons, New York, 1997.
[25] B. Reppich, in: R.W. Cahn, P. Hassen, E.J. Kramer (Eds.), Materials Science and Technology: A Comprehensive Treat-ment, vol. 6, VCH, Weinheim, 1993, p. 311.
[26] J.F. Nie, Scripta Materialia 48 (2003) 1009−1015.
[27] J.S. Chun, J.G. Byrne, Journal of Materials Science 4 (10) (1969) 861−872.
[28] E.O. Hall, Proceedings of the Physical Society, Section B 64 (1951) 747−753.
[29] Cheng Zhenhua, Wrought Magnesium Alloy [M], Chemical Industry Press, Beijing, 2005, p. 6.
[30] Yasumasa Chino, Motohisa Kado, Mamoru Mabuchi, Materials Science and Engineering A 494 (2008) 343−349.
[31] J. Koike, T. Kobayashi, T. Mukai, H. Watanabe, M. Suzuki, K. Maruyama, K. Higashi, Acta Materialia 51 (2003) 2055−2065.